Academic Journal of Science and Technology
ISSN: 2771-3032 | Vol. 20, No. 3, 2026

A Low-Profile High-Isolation Duplex Antenna with Omnidirectional and Unidirectional Radiation Patterns

Wei Wang

School of Physics & Optoelectronic Engineering, Guangdong University of Technology, Guangzhou, Guangdong, 510006, China

Abstract: In this paper, a low-profile high-isolation duplex antenna operating at 3.6/4.5 GHz is proposed for 5G wireless communication systems. The proposed antenna has a low profile of 0.06λ_0 at 3.6 GHz and a single circular radiator, which is coupled excited by two high-isolation ports simultaneously for duplexing application. When Port 1 is excited, a -10 dB impedance bandwidth with omnidirectional radiation is obtained to cover N78 band. When Port 2 is excited, a -10 dB impedance bandwidth with unidirectional radiation is achieved for covering N79 band. Due to the different feeding schemes and orthogonal radiation patterns, the in-band isolation both for the two operation bands is higher than 35 dB without additional decoupling structure. The proposed antenna is fabricated and measured. The simulated and the measured results are in a good agreement. Results show that the -10 dB impedance bandwidths for the two ports are 3.24–3.95 GHz and 4.33–5.37 GHz, respectively, and the gains for the two operation bands are 2.7–5.15 dBi and 8.8–11.1 dBi, respectively.

Keywords: Antenna; Duplex Antenna; High Isolation; Omnidirectional Radiation; Unidirectional Radiation.

1. Introduction

With the rapid development of the Internet of Things (IoT) and intelligent terminals, the wireless communication systems have put forward increasingly stringent requirements of antennas with multi-functional integration and miniaturization. In complex wireless communication environments, the omnidirectional radiation mode is required to ensure wide-area signal coverage, while the unidirectional radiation mode is dedicated to improving the gain and anti-interference capability of long-distance transmission, so antenna with a single radiation mode can no longer meet diverse transmission requirements. Meanwhile, the antenna with duplex characteristic enables simultaneous transmission of transmitted and received signals, which can greatly improve communication efficiency. Therefore, duplex antenna with both omnidirectional and unidirectional modes have become core device to adapt to the needs of multi-scenario communication.

In the practical application, low profile and high isolation are required by duplex antenna. The low-profile feature enables the duplex antenna to be flexibly integrated into various lightweight intelligent devices, base station terminals, and vehicle-mounted communication systems, and that is in line with the miniaturization design trend of modern electronic equipment. High isolation is important for suppressing electromagnetic interference between receiving and transmitting signal channels, as well as ensuring the purity of signal transmission and system stability. Insufficient isolation performance will directly lead to signal crosstalk and increased bit error rate, and that will seriously affect communication quality. However, the design of traditional dual-mode duplex antennas often faces many technical difficulties. To switch omnidirectional and unidirectional modes, complex feeding network or reconfigurable structure is usually required, which not only increase the profile and volume of the duplex antenna, but also introduce additional insertion loss. At the same time, the integration of duplex function and dual-mode characteristics will aggravate the electromagnetic coupling between ports, making that high port-to-port isolation is difficult to be achieved.

Researchers have made some progress in improving the performance of dual-mode duplex antennas by optimizing antenna topology, innovating feeding mechanisms, and introducing new decoupling technologies. Some designs rely on the low-profile advantage of microstrip patch antennas, combined with Characteristic Mode Analysis (CMA), to realize the switching between monopole-like omnidirectional and unidirectional dual modes [1]-[4].The TM_{01} mode in this structure has similar characteristics to the lowest mode of the monopole patch antenna, and its working principle has been studied through Characteristic Mode Analysis (CMA)[1]and cavity model analysis[2].Based on CMA theory, the electric field distribution of the patch antenna excites the directional radiation mode of TM11 mode on the circular patch antenna[4].To mitigate port-to-port coupling in duplex antennas, extensive research has been conducted using various techniques, including orthogonal polarization [5], defected ground structure (DGS) [6], metasurface [7], neutralization line [8], and parasitic resonators [9]. Some of the existing designs meet the requirements of low profile and high isolation, but still have problems, such as narrow bandwidth and complex switching mechanisms. There are still some designs, which have dual modes, but sacrifice duplex flexibility or integration, and they are difficult to adapt to the core requirements of multi-band and high integration in practical systems.

This paper proposes an dual-mode (omnidirectional and unidirectional radiation patterns) duplex antenna with low profile, high isolation, wide operating bandwidth, and a simple switching mechanism. The low operating band with omnidirectional radiation is 3.24-3.95 GHz, and the high operating band with unidirectional radiation is 4.33–5.37 GHz. Within the two operating bands, the antenna gain is stable, and the port-to-port isolation exceeds 35 dB. Both simulated and measured results validate that the proposed antenna is well-suited for wireless communication duplexing systems.

2. Structure of the Proposed Low-Profile High-Isolation Duplex Antenna

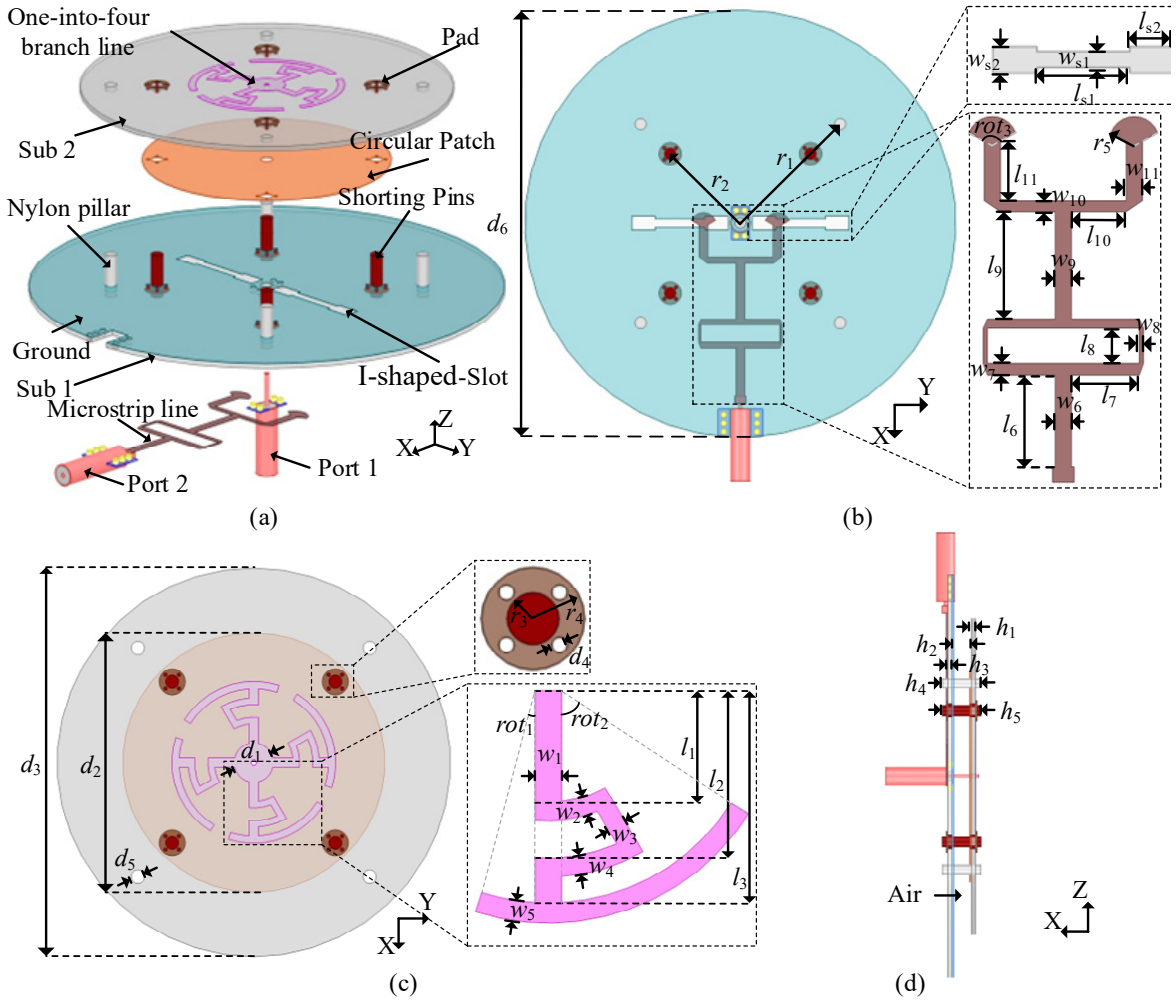


Fig 1. Configuration of the proposed antenna, (a) Perspective view, (b) top and bottom views of Sub 1, (c) top and bottom views of Sub 2, (d) side view

The structure of the proposed antenna is shown in Fig.1. Sub 1 and Sub 2 are used to design the proposed antenna, and both Sub 1 and Sub 2 are Arlon 25FR substrates (Arlon 25FR TM, ε_r = 3.58, tan δ = 0.0035) with a thickness of h_1 = h_3 =0.762 mm. There is an air layer with thickness of h_2 = 3.5 mm between Sub 1 and Sub 2, as shown in Fig.1(d). Sub 1 and Sub 2 are supported by four nylon pillars with a diameter of d_5 = 2 mm and a height of h_4 = 7.1 mm. The total profile height of the proposed antenna is h_1+h_2+h_3 = 5.024 mm, which is about 0.06λ_0 at 3.6 GHz.

A circular ground plane and a feeding microstrip line are printed respectively on the top and the bottom layers of Sub 1, as shown in Figs.1(a).There is a pair of symmetrical I-shaped slots etched into the ground, the feeding microstrip line is connected to port 2, and the port 1 is placed in the center of the ground. The detailed dimensions of the slots and the microstrip line are given in Fig.1(b). A circular radiation patch with a diameter of d_2 = 20 mm is printed on the bottom layer of Sub 2, as shown in Fig.1(a), and it is short to the ground plane through four shorting pins. As shown in Figs.1(a) and 1(c), each of the shorting pins with a height of h_5 = 7.2 mm has two annular pad (one is placed on the upper surface of Sub 2, and the other one is placed on the bottom surface of Sub1), and a copper pillar. A metal disk with a diameter of d_1 = 6 mm and folded arc-shaped branch lines distributed in a one-into-four sequential rotation structure is printed on the upper surface of Sub 2, and the detail dimensions of the metal disk are shown in Fig.1(c). A small hole is placed in the center of the metal disk, which is connected to port 1 through the coaxial probe of a Sub-Miniature Version A (SMA) connector. The energy from port 1 is transmitted to the one-into-four branch lines, and then coupled to the circular patch, realizing the monopole-like pattern, with omnidirectional radiation within the low operating band. The pair of I-shaped slots are perpendicular to the folded feeding microstrip line, and the energy from the feeding microstrip line coupled fed the circular patch through the I-shaped slots, realizing the unidirectional radiation pattern, within the high-frequency operating band.

All physical dimensions of the proposed antenna are listed in Table 1.

Table 1. All physical dimensions of the proposed antenna (unit: mm/deg)

h_1	h_2	h_3	h_4	h_5	d_1	d_2	d_3	d_4	d_5	d_6
0.762	3.5	0.762	7.1	7.2	6	40	60	0.6	2	76.4
l_1	l_2	l_3	l_6	l_7	l_8	l_9	l_{10}	l_{11}	l_{s1}	l_{s2}
6.0	9.0	11.4	8.6	6.3	3.3	10.1	5.1	5.6	8.8	4.15
w_1	w_2	w_3	w_6	w_7	w_8	w_9	w_{10}	w_{11}	w_{s1}	w_{s2}
1.4	1	1	1.5	1.1	0.4	1.5	1	1.5	1.6	2.6
w_4	w_5	r_1	r_2	r_3	r_4	r_5	rot_1	rot_2	rot_3	
1	1.1	25	17.6	1	2	2.3	20	56	120	

Note: rot_1, rot_2, and rot_3 are rotation angle parameters with the unit of degrees.

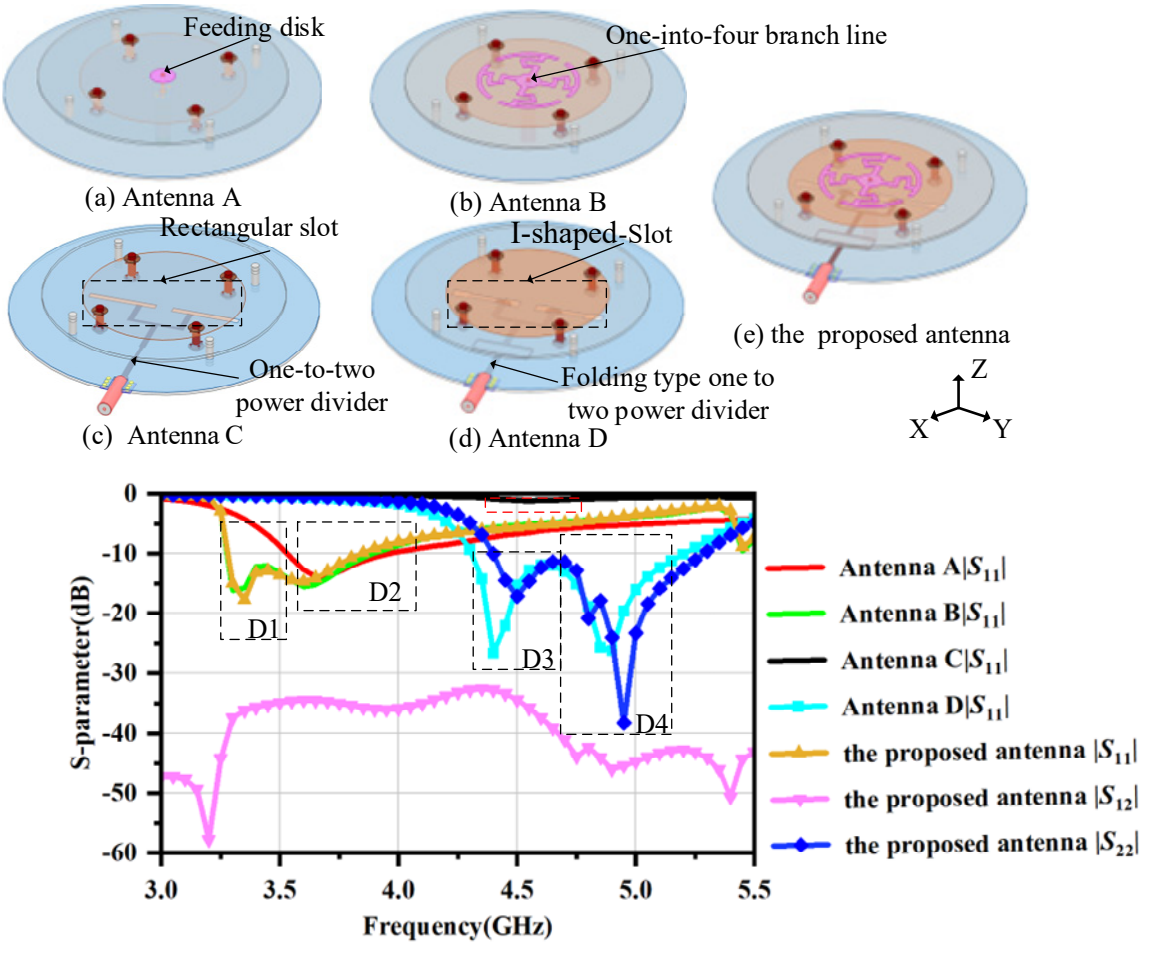
3. Working Principle Analysis of the Proposed Antenna

3.1. Analysis of the Antenna Design and Evolution Process

Fig.2 shows the evolution process of the proposed low-profile high-isolation duplex antenna with omnidirectional and unidirectional radiation patterns, as well as a comparison of the S-parameters of the reference antennas.

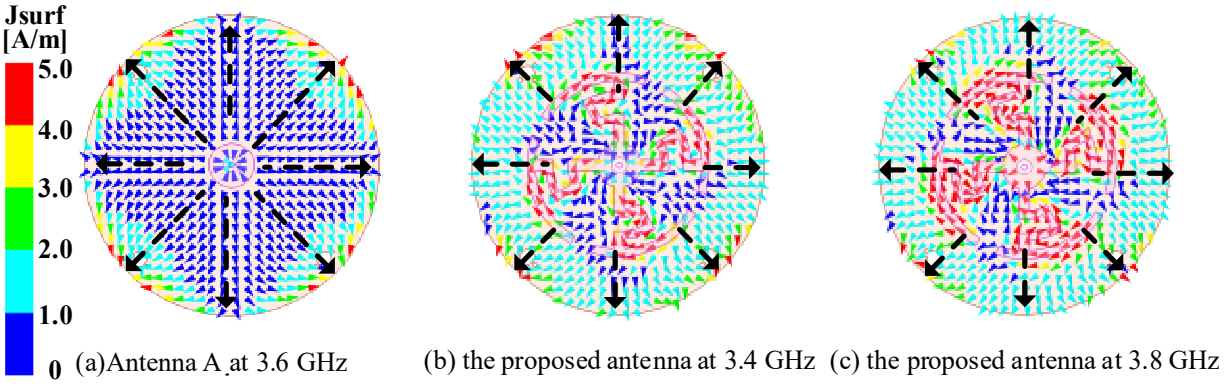
In the research of traditional patch antennas, a monopole-like radiation mode can be realized by introducing shorting pins into the circular patch antenna. This radiation mode is the TM_{01} mode, which can generate omnidirectional radiation. Antenna A, shown in Fig.2 (a), is a monopole-like antenna with a disk-coupled feed. For Sub 1 of Antenna A, a feeding disk printed on the upper surface and a circular radiation patch printed on the lower surface, four shorting vias are used to short-circuit the circular patch to the ground plane. The radius of the circular radiation patch d_2 = 20 mm, which is close to the 1/4 wavelength in free space at 3.7 GHz, thus exciting the TM_{01} resonant mode at this frequency, as shown in Fig.2 (f).

The current distribution under this resonant mode is shown in Fig.3 (a). When Antenna A operates at 3.6 GHz, the disk-coupled feed is adopted, and the current density at the center of the circular patch is the minimum, almost zero. This is because in the TM_{01} mode, the electric field is asymmetrically distributed on the central axis, while the current is related to the change rate of the electric field. The low change rate of the electric field at the center leads to a small current density. The direction of the current vector is along the radial direction, and the current density increases gradually from the center to the edge of the patch, reaching the maximum at the edge of the patch, which is the typical current characteristic of the TM_{01} mode. An omnidirectional radiation mode can be realized in this working mode.



(f) S-parameters of antenna evolution process

Fig 2. Design process of the proposed antenna



(a)Antenna A at 3.6 GHz (b) the proposed antenna at 3.4 GHz (c) the proposed antenna at 3.8 GHz

Fig 3. Current distribution on circular patch in omnidirectional radiation mode

Based on the theoretical analysis of circular patch antennas [1] and [2], the introduction of a parasitic structure at the feeding disk can effectively broaden the operating bandwidth of the antenna. The structure with one-into-four sequential rotation branch lines can not only ensure the stability of gain and radiation pattern in the omnidirectional radiation mode, but also further expand the bandwidth. As shown in Fig.3, after adding the parasitic structure, two resonant modes are finally formed at 3.4 GHz and 3.7 GHz in the omnidirectional radiation working mode, denoted as D1 and D2, respectively.

From the perspective of current, when the antenna designed in this chapter operates at 3.4 GHz and 3.7 GHz, the current distribution on the one-into-four sequential rotation branch lines presents a multi-lobe rotationally symmetric form. This distribution characteristic enables the radiation field components of the patch in all directions of the horizontal plane to be synthesized with equal amplitude through spatial superposition. Finally, a radially distributed current is generated at the outer ring without the feeder line, which is similar to the external current direction of Antenna A at 3.6 GHz, and ultimately achieves 360° uniform radiation characteristics in the horizontal plane under the omnidirectional radiation mode. As shown in Fig.2 (f), after introducing the one-into-four sequential rotation branch lines, the impedance matching of Antenna B is much better than that of Antenna A, achieving a -10 dB operating frequency band from 3.30 GHz to 3.85 GHz. The radiation pattern at 3.4 GHz in this frequency band is depicted in Fig.4 (a), and the antenna presents an omnidirectional radiation mode covering the band N78.

Based on the CMA theory, a detailed analysis of the working mode of circular microstrip patch antennas was conducted in [4]. By utilizing the inherent field distribution characteristics of its main mode TM_{11}, directional radiation of the antenna was achieved, providing an important reference for the design and optimization of directional radiation modes of patch antennas. To obtain the second directional working mode and ensure port symmetry, two symmetrically distributed rectangular slot structures are introduced along the y-axis on the ground plane, and a two-way equal-split microstrip power divider connected to port 2 is designed and printed on the bottom layer of Sub 1, with the structure shown in Fig.1 (c). The length of the rectangular slot is 17.1 mm, corresponding to 1/4 wavelength at 4.39 GHz, so that Antenna C generates a resonance point at 4.6 GHz, as shown in Fig.2 (f).

To further expand the operating bandwidth of the antenna, the structure of the rectangular slot and the two-way microstrip power divider is optimized: the rectangular slot is replaced with an I-shaped slot, the end of the microstrip line is replaced with a fan-shaped structure with a rotation angle of $rot_3 = 120°$, and the microstrip line is folded. Finally, two resonant modes are formed at 4.5 GHz and 4.9 GHz, denoted as D3 and D4, respectively, as shown in Fig.2 (f). The optimized Antenna D has better impedance matching characteristics, achieving a -10 dB impedance bandwidth in the range of 4.35 GHz to 5.20 GHz. As shown in Fig.5 (a), at 4.5 GHz, the currents along the I-shaped slot on the upper and lower sides of the ground plane are in opposite phase, resulting in radiation cancellation, while the directions of the strong currents distributed on the left and right edges of the I-shaped slot are the same, which proves that the dipole resonant mode is excited. The uncanceled current on the ground plane transmits energy to the circular patch through coupling, as shown in Fig.4 (b). The radiation pattern at 4.5 GHz is shown in Fig.4 (b), and the maximum gain in this working mode can reach more than 10 dB.

The proposed low-profile high-isolation duplex antenna with omnidirectional and unidirectional radiation characteristics in this chapter is shown in Fig.2 (e). The antenna is composed of Antenna B operating in omnidirectional radiation mode and Antenna D operating in the unidirectional radiation mode. The two working modes adopt independent feeding networks and share the same circular radiation patch. It can be seen from Fig.2 (f) that the operating frequency band of the combined antenna when port 1 is excited is basically consistent with that of Antenna B, and the operating frequency band when port 2 is excited is highly consistent with that of Antenna D.

Combined with the radiation pattern shown in Fig.4, it can be seen that when port 1 is excited, the antenna presents monopole-like omnidirectional radiation characteristics at 3.4 GHz, and its gain reaches the minimum in the positive direction of the z-axis; when port 2 is excited to form unidirectional radiation, the maximum gain appears in the positive direction of the z-axis, and the gain in other directions is low. The proposed duplex antenna realizes the diversification of radiation patterns through two ports, effectively suppresses the spatial wave coupling, and thus reduces the mutual coupling between ports. Based on the above mechanism, the port isolation of the duplex antenna can reach more than 35 dB.

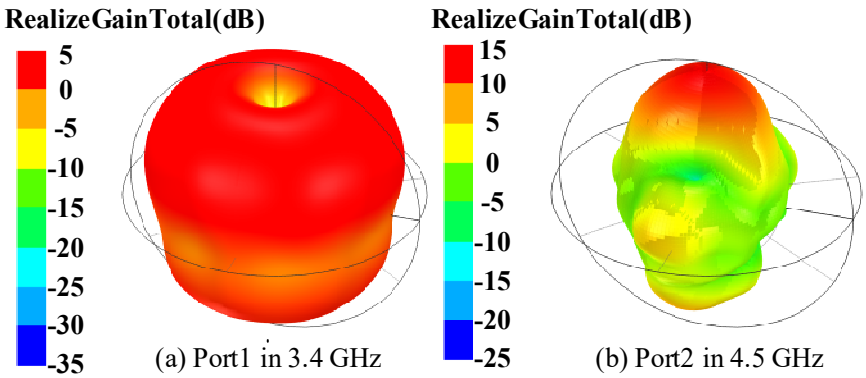


Fig 4. Three-dimensional radiation pattern of the proposed duplex antenna

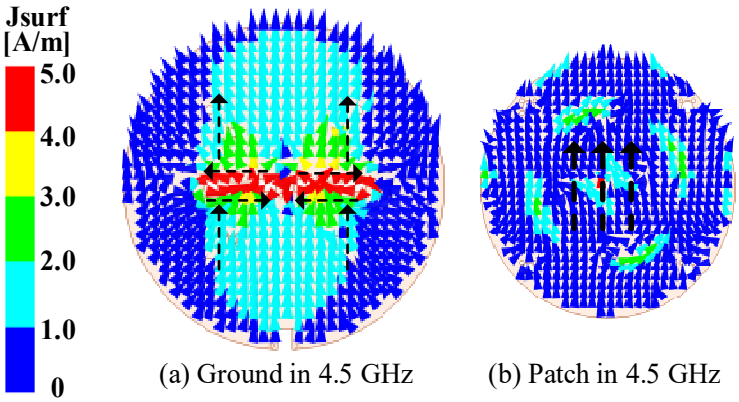


Fig 5. Current distribution of the unidirectional mode feed network under different operating modes

3.2. Analysis of Operating Frequency Band Tuning

The research on the working mode of the circular microstrip disk antenna with an air gap has been very mature. Early research by R. Garg in [10] revealed that the core of the circular microstrip disk antenna is to use the air layer to tune the resonant frequency and expand the bandwidth. According to the research proposed by Juhua Liu in [11], when the circular patch is not short-circuited by metal conductive vias, the resonant frequency of the lowest-order mode (TM_{01} mode) is 0; to make the TM_{01} mode produce a non-zero resonant frequency, metal shorting vias must be introduced.

The antenna, when port 1 operates in the omnidirectional radiation mode, in this chapter, refers to the basic design model of the circular microstrip disk antenna. First, the physical radius of the circular patch is corrected for the edge field effect through formula (1), and the equivalent electrical size radius R_{eff} of the antenna is obtained, where H is the thickness of the Substrate, and εr is the relative permittivity of the Substrate. On this basis, the resonant frequency f_{TM01} of the TM_{01} mode that can be excited after loading the shorting vias can be calculated by formula (2), where c is the speed of light in vacuum, 0 and 1 are the mode order indices along the circumferential angle direction and the radial direction, respectively, and $\chi_{01} = 2.04048$ is the first positive root of the 0th-order Bessel function of the first kind $J_0(x)$, which is the characteristic constant of the TM_{01} mode in cylindrical waveguides and resonant cavities.

In the design of this chapter, the physical radius of the circular patch R = 20 mm, the thickness of the substrate H = 0.762 mm, and the relative permittivity of the medium ε_r = 3.58. The equivalent radius R_{eff} corrected by formula (1) is 20.37 mm; substituted into formula (2), the calculated resonant frequency of the TM_{01} mode is 3.39 GHz, which is in good agreement with the electromagnetic simulation results of Antenna A, as shown in Fig.2 (f).

$$R_{eff} = R\sqrt{1+\frac{2H}{\pi R\varepsilon_r}\left(\ln\frac{\pi R}{2H}+1.7726\right)} \tag{1}$$

$$f_{\text{TM01}} = \frac{\chi_{01}\cdot c}{2\pi R_{eff}\sqrt{\varepsilon_r}} \tag{2}$$

Based on the establishment of the basic model of the circular patch antenna, the parameters that affect the core performance of the antenna in this chapter are further analyzed, as shown in Fig.6. In the above calculation, the physical radius R of the circular patch is greatly correlated with the resonant frequency of the antenna. As shown in Fig.6 (a), the diameter d_2 of the circular patch is scanned. As d_2 increases from 38.0 mm to 42.0 mm, the second resonant point D2 when port 1 is excited shifts to a lower frequency, which has the same change trend as formula (2). Since ports 2 and port 1 share the same radiator, when port 2 is excited, the operating frequency band of port 2 also shifts to a lower frequency as d_2 increases.

When port 1 is excited, the omnidirectional radiation working mode has two resonant modes, denoted as D1 and D2. The resonant mode D1 is very sensitive to the parameters of the one-into-four sequential rotation branch lines. As shown in Fig.6 (b), taking the diameter d_1 of the feeding disk as an example, by increasing d_1, the resonant mode D1 shifts to a lower frequency, while D2, which is greatly affected by the radiation patch, does not change much with the variation of d1. In addition to the patch and feeding network, the shorting vias that can generate the non-zero resonant frequency of the TM_{01} mode also have a great influence on the operation of the resonant mode D2. As shown in Fig.6 (c),

the position r1 of the shorting vias has little correlation with the resonant mode D1 but has a great correlation with the resonant mode D2. By selecting an appropriate shorting via position r_1 = 17.6 mm or r_1 = 18.1 mm, $|S_{11}|$ <- 10 dB can be achieved in the N78 operating frequency band.

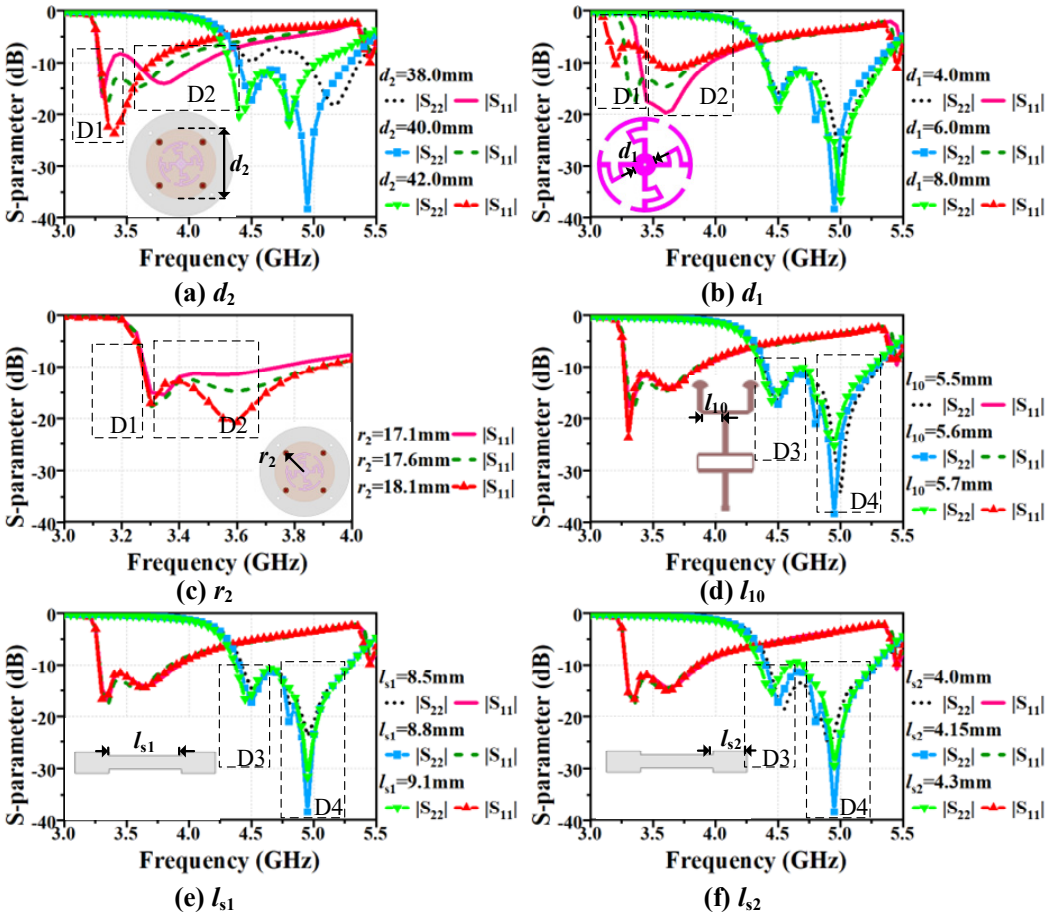


Fig 6. Simulated S-parameters of the proposed antenna vary with different dimensions

When port 2 is excited, the unidirectional radiation working mode also has two resonant modes, denoted as D3 and D4. The coupling position between the feeding microstrip line and the I-shaped slot is sensitive to the resonant mode D4. As shown in Fig.6 (d), as l_{10} increases, the resonant mode D4 shifts to a lower frequency, while the operating frequency band of the resonant mode D3 is almost unaffected by l_{10}. The coupling strength between the radiation patch and the feeding microstrip line depends on the size of the I-shaped slot, so D3 is very sensitive to the values of ls_1 and ls_2. As shown in Fig.6 (e) and (f), by increasing ls_1 or ls_2, the operating frequency band of port 2 shifts to a lower frequency, and vice versa. However, the operating frequency band of port 1 is almost unaffected by l_{10}, ls_1, and ls_2, which is due to the design of the radiation pattern diversity between the two ports, thus realising independent tuning between ports.

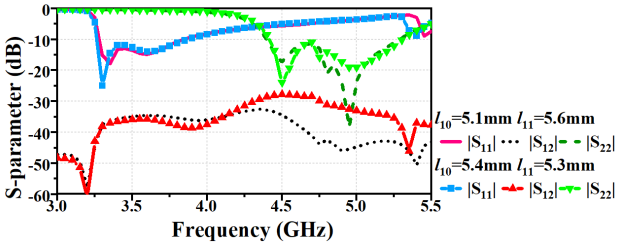


Fig 7. Simulated S-parameters of the proposed antenna in this chapter vary with l_{10} and l_{11}

Based on the above analysis, the operating frequency bands of port 1 and port 2 can be adjusted by adjusting the sizes of the circular patch, feeding disk, feeding microstrip line, and I-shaped slot, respectively. Among them, the isolation between ports is relatively sensitive to the coupling position between the feeding microstrip line and the I-shaped slot. As shown in Fig.7, although D3 and D4 are located in the operating frequency band of port 2 at different coupling positions, there is still a gap of nearly 10 dB in the in-band isolation. When l_{10} = 5.1 mm and l_{11} = 5.6 mm, the proposed antenna has two operating frequency bands (3.30 GHz to 3.85 GHz and 4.35 GHz to 5.20 GHz) with an isolation greater than 35 dB, which can meet the application requirements of both in-band full-duplex and frequency division duplex communication modes in 5G systems.

3.3. Analysis of High Isolation Mechanism

In a duplex system, low interference between the transmitting and receiving channels is critical, so the duplex antenna needs to have high isolation characteristics from port to port. The proposed antenna achieves a high isolation of 35 dB due to the following four reasons: (1) The two ports of the antenna operate in different frequency bands; (2) Different feeding technologies are adopted for the two ports; (3) The polarizations of the two ports of the proposed antenna are orthogonal; (4) Radiation pattern diversity technology is adopted between the two ports.

From the perspective of polarization, the TM_{11} unidirectional mode and the TM_{01} omnidirectional mode of the circular microstrip patch antenna have inherent

polarization orthogonality. The electric field of the TM_{11} main mode is distributed along the tangential direction of the patch circumference, presenting linearly polarized radiation in space, and the pattern has obvious directivity. The electric field of the TM_{01} mode is distributed along the radial direction of the patch, corresponding to vertical polarization, which can form omnidirectional radiation in the horizontal plane. Since the radial and tangential directions are perpendicular to each other in the geometric structure, the electric field vectors of the two modes are orthogonal to each other, thus realizing orthogonally polarized radiation and providing high inter-port isolation for the dual-polarized antenna.

From the perspective of the radiation pattern, as shown in Fig.4, when port 1 is excited, the monopole-like omnidirectional radiation pattern at 3.6 GHz has the minimum gain in the positive direction of the z-axis. When port 2 is excited to generate unidirectional radiation, the maximum gain is in the positive direction of the z-axis, and the gain gradually decreases when deviating from the positive direction of the z-axis. Therefore, the two ports of the proposed duplex antenna realise pattern diversity, which helps to improve the isolation between ports.

From the perspective of current, as shown in Fig.5, when port 2 is excited, the currents distributed in the two I-shaped slots have a phase difference of 180°, so the equivalent current at the feeding position of port 1 is almost zero. As shown in Fig.8, when excited at 4.5 GHz, the current distributed on the one-into-four sequential rotation branch lines is basically less than 1 A/m, which can be ignored, resulting in an inter-port isolation higher than 40 dB in the range of 4.6 GHz-5.2 GHz. Similarly, when port 1 is excited, the current is mainly concentrated on the one-into-four sequential rotation branch lines. Due to the low profile of the antenna, the current is transmitted to the microstrip line through the I-shaped slot by the coupling effect. After two times of current synthesis on the microstrip line, the current reaching port 2 is very weak due to the current cancellation effect, thus achieving an isolation of 35 dB in the low frequency band.

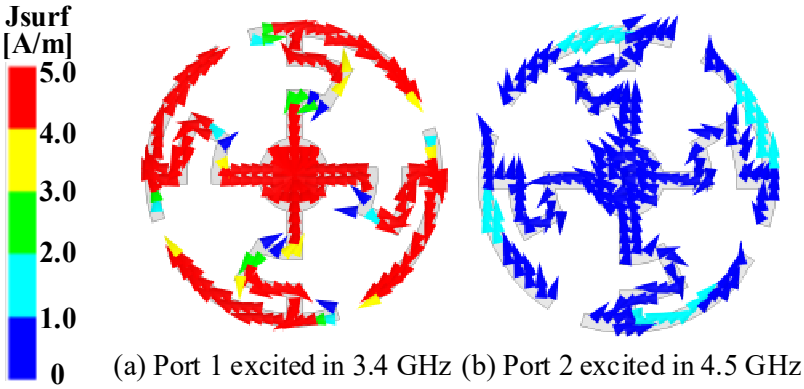


Fig 8. Current distribution of the feed network under the omnidirectional mode

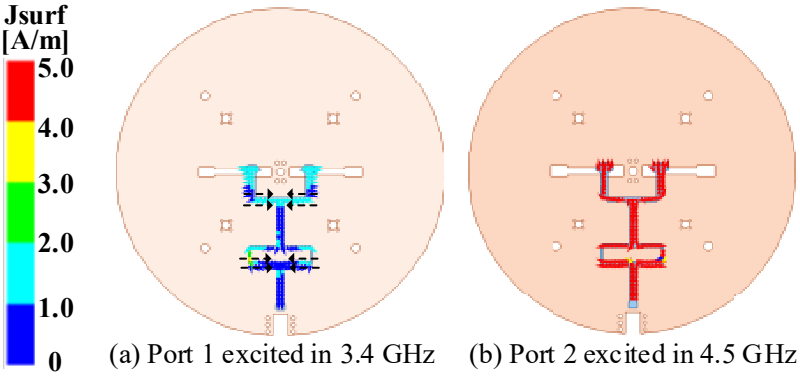


Fig 9. Current distribution of the feed network under the unidirectional mode

4. Measured Results of the Proposed Antenna

To verify the performance of the designed low-profile high-isolation duplex antenna with omnidirectional and unidirectional radiation modes, an antenna prototype was fabricated and measured in a near-field measurement system in a microwave anechoic chamber. The measurement environment and physical photos of the prototype are shown in Fig.10. The measured S-parameters, gain, and efficiency results of the antenna are shown in Fig.11.

In the simulation results, the antenna achieves operating bandwidths of 3.30-3.85 GHz and 4.40-5.25 GHz, with an inter-port isolation higher than 35 dB. The gain of port 1 in the omnidirectional radiation mode is 2.7-5.15 dBi, and the gain of port 2 in the unidirectional radiation mode is 8.8-11.1 dBi. The measured results show that the two different operating frequency bands of the proposed antenna are 3.24-3.95 GHz and 4.33-5.37 GHz, respectively, and the isolation between the upper and lower operating frequency bands is 39.5 dB and 35 dB, respectively, as shown in Fig.11 (a).

When port 1 is excited, a flat in-band gain (about 4.0 dBi) is achieved in the omnidirectional radiation mode, as shown in Fig.11 (b). When port 2 is excited, the measured in-band gain in the unidirectional radiation mode is 6.0 to 8.0 dBi, as shown in Fig.11 (b). The in-band radiation efficiencies of port 1 and port 2 are higher than 80% and 60%, respectively. The overall trend of the measured results is consistent with the simulation results, but there is a certain error in the numerical value, which is mainly caused by two aspects: the

manufacturing process and the measurement environment.

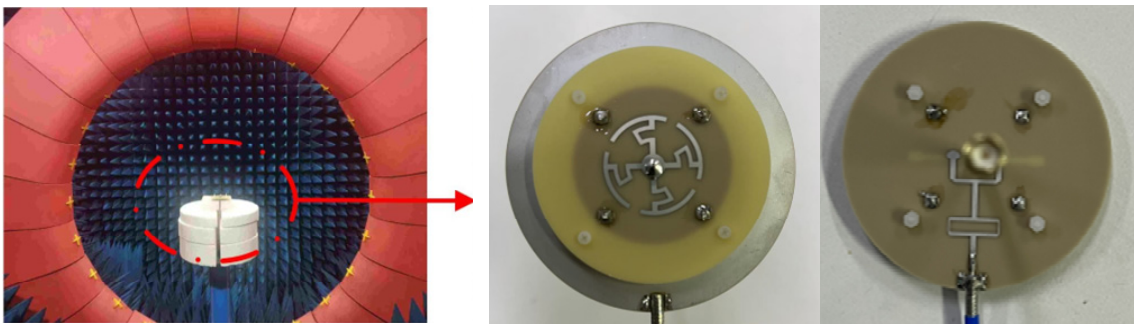
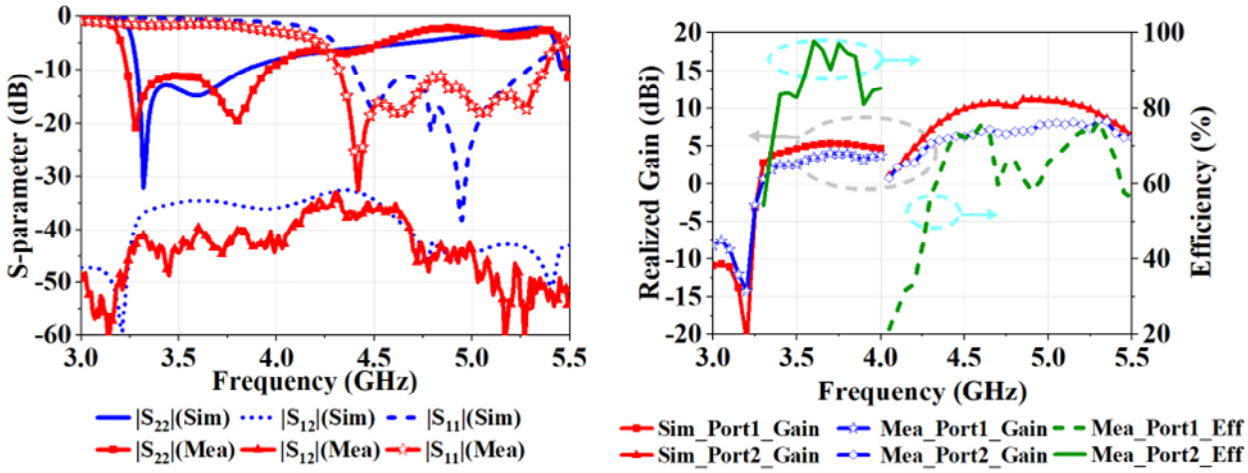


Fig 10. The measurement environment and prototype of the fabricated antenna.



(a) S-parameters (b) Gain and Efficiency

Fig 11. Simulated and measured results of the proposed antenna.

The simulated and measured normalized radiation patterns of the antenna at different planes and frequencies are shown in Fig.12. When port 1 operating in the omnidirectional radiation mode is excited, two representative frequency points of 3.4 GHz and 3.7 GHz are selected for measurement. The antenna presents an omnidirectional radiation pattern on the XOY plane, with a cross-polarization level less than -10 dB. When port 2 operating in the unidirectional radiation mode is excited, two frequency points of 4.5 GHz and 5.0 GHz are selected for measurement. The antenna presents a unidirectional radiation pattern in the broadside direction, with a cross-polarization level less than -20 dB.

The simulation results of the antenna proposed in this chapter are compared with those of other reported duplex antennas in Table 2. Although the antennas reported in references [14] and [17] have a profile height of less than 0.05λ_0, their antenna bandwidth is relatively narrow. The antenna in this chapter has more advantages in gain in both omnidirectional and unidirectional modes compared with the literature in Table 2. The antennas in references [16] and [18] can realize pattern diversity (omnidirectional and unidirectional radiation modes) like the antenna proposed in this paper, but the antenna in this chapter has a wider operating bandwidth and higher isolation. In summary, the proposed dual-mode duplex antenna has comprehensive advantages in key performance indicators such as bandwidth, inter-port isolation, and profile height, so it is more suitable for practical wireless communication duplex systems.

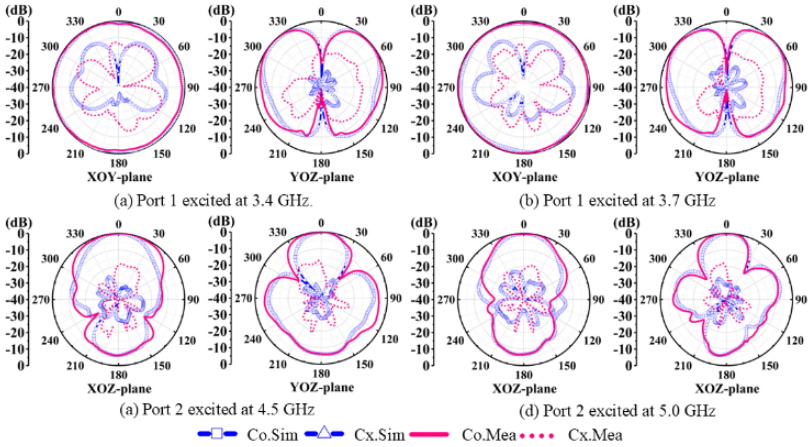


Fig 12. Simulated and measured normalized radiation patterns of the proposed antenna

Table 2. Performance Comparison of the Proposed Antenna with Other Duplex Antennas

Ref.	Profile. (λ_0)	Port	IBW (%)	Iso. (dB)	Polarization	Rad. Patt.	Gain (dBi)
[12]	0.28	2	24.0/11.8	23/25	LP	Uni.	7.5/7.6
[13]	0.06	2	4.9/6.1	44/41	LP	Uni.	8.5/9.5
[14]	0.013	2	2.1/1.5	47/45	LP	Uni.	2.9/1.23
[15]	0.14	2	6.8/8.0	40	LP	Uni./ Uni.	5.2/8.0
[16]	0.06	3	8.1/7.3	30	CP/ LP	Omni./ Uni.	2.0/11.0
[17]	0.03	3	6.4/6.9/8.8	30	LP	Omni./ Uni./ Uni.	3.4/8.6/8.5
Pro.	0.05	2	15.4/17.6	35	LP	Omni./ Uni.	5.1/11.1

Note: λ_0 is the free-space wavelength at the lower edge frequency.

5. Summary

In this chapter, a low-profile high-isolation duplex antenna with omnidirectional and unidirectional radiation modes has been studied in this letter. Through the differential feeding design of dual ports, the antenna adopts a one-into-four sequential rotation branch line coupled feed at port 1 to excite the TM_{01} mode of the circular patch for omnidirectional radiation; at port 2, a one-to-two microstrip line coupled with I-shaped slots loaded on the ground plane is used to excite the TM_{11} mode for unidirectional radiation. The operating frequency bands of the dual ports of the antenna support independent tuning, which can be flexibly adapted to the inter-frequency duplex scenario, providing a feasible engineering scheme for the design of multi-mode integrated duplex antennas.

References

[1] L. Y. Nie, B. K. Lau, S. Xiang, H. Aliakbari, B. Wang and X. Q. Lin, Wideband Design of a Compact Monopole-Like Circular Patch Antenna Using Modal Analysis. IEEE Antennas and Wireless Propagation Letters. 2021, Vol. 20 (No. 6), p. 918-922.

[2] J. Liu, Q. Xue, H. Wong, H. W. Lai and Y. Long, Design and Analysis of a Low-Profile and Broadband Microstrip Monopolar Patch Antenna. IEEE Transactions on Antennas and Propagation. 2012, Vol. 61 (No. 1), p. 11-18.\

[3] B. Jecko and C. Decroze, The 'monopolar wire patch antenna' concept. Proc. 2nd Eur. Conf. Antennas and Propagation (EuCAP). 2007, p. 1-5.

[4] P. Sumithra and D. Kannadassan, Characteristic Mode Analysis of Circular Microstrip Patch Antennas. 2018 IEEE Indian Conference on Antennas and Propagation (InCAP). Hyderabad, India, 2018, p. 1-4.

[5] Y. Li, Z. Zhang, Z. Feng and M. F. Iskander, "Dual-Mode Loop Antenna With Compact Feed for Polarization Diversity," IEEE Antennas and Wireless Propagation Letters, no. 10 (2011): 95-98.

[6] C. Y. Chiu, C. H. Cheng, R. D. Murch and C. R. Rowell, "Reduction of Mutual Coupling Between Closely-Packed Antenna Elements," IEEE Transactions on Antennas and Propagation 55, no. 6 (2007): 1732-1738.

[7] Y. F. Cheng, X. Ding, W. Shao and B. Z. Wang, "Reduction of Mutual Coupling Between Patch Antennas Using a Polarization-Conversion Isolator," IEEE Antennas and Wireless Propagation Letters 16, (2017): 1257-1260.

[8] A. Diallo, C. Luxey, P. Le Thuc, R. Staraj and G. Kossiavas, "Study and Reduction of the Mutual Coupling Between Two Mobile Phone PIFAs Operating in the DCS1800 and UMTS Bands," IEEE Transactions on Antennas and Propagation 54, no. 11 (2006): 3063-3074.

[9] S. C. Chen, Y. S. Wang and S. J. Chung, "A Decoupling Technique for Increasing the Port Isolation Between Two Strongly Coupled Antennas," IEEE Transactions on Antennas and Propagation 56, no. 12 (2008): 3650-3658.

[10] R. Garg, P. Bhartia, I. Bahl, and A. Ittipiboon, Microstrip Antenna Design Handbook. Artech House, 2001, p. 314-320.

[11] J. Liu, Q. Xue, H. Wong, H. W. Lai and Y. Long, Design and Analysis of a Low-Profile and Broadband Microstrip Monopolar Patch Antenna. IEEE Transactions on Antennas and Propagation. 2013, Vol. 61 (No. 1), p. 11-18.

[12] H. Yuan, F. C. Chen and K. R. Xiang, A Sub-6 GHz Dual-Band Dual-Polarized Filtering Antenna. IEEE Antennas and Wireless Propagation Letters. 2025, Vol. 24 (No. 4), p. 908-912.

[13] T. H. Bui, H. T. Vu, S. X. Ta, K. K. Nguyen, C. Dao-Ngoc and N. Nguyen-Trong, Dual-Band Dual-Polarized Slotted-Patch Antenna for In-Band Full-Duplex Applications. IEEE Antennas and Wireless Propagation Letters. 2023, Vol. 22 (No. 6), p. 1286-1290.

[14] D. P. Purbey, S. Ghosal and A. De, Shorting-Pin-Inspired Coupling Reduction in Dual-Band Dual-Polarized STAR Antenna. IEEE Antennas and Wireless Propagation Letters. 2025, Vol. 24 (No. 1), p. 43-47.

[15] M. Yadav, S. Maithani, V. Sangwan and R. K. Gangwar, Dual-Band Full-Duplex Compact Antenna for Vehicular Application. 2023 IEEE Microwaves, Antennas, and Propagation Conference. 2023, p. 1-5.

[16] C. X. Mao, D. H. Werner, Y. Zhang and X. -Y. Zhang, Compact Dual-Band Dual-Mode Antenna With Omni-/Unidirectional Radiation Characteristics. IEEE Antennas and Wireless Propagation Letters. 2019, Vol. 18 (No. 12), p. 2657-2660.

[17] T. H. Bui, S. X. Ta, K. K. Nguyen, C. Dao-Ngoc and N. Nguyen-Trong, Planar High-Isolation Dual-Band Dual-Mode Antenna With Omni-/Unidirectional Radiation. IEEE Antennas and Wireless Propagation Letters. 2021, Vol. 21 (No. 1), p. 99-103.